

SIMULATION OF BOUNDARY LAYER CLOUDS WITH DOUBLE-MOMENT MICROPHYSICS AND MICROPHYSICS-ORIENTED SUBGRID-SCALE MODELING

D. Jarecka¹, W. W. Grabowski², H. Morrison², H. Pawlowska¹,
J. Slawinska¹ and A. A. Wyszogrodzki²

¹ Institute of Geophysics, University of Warsaw, Warsaw, Poland

² National Center for Atmospheric Research, Boulder, Colorado, USA

1. INTRODUCTION

Mixing of cloud with dry environmental air changes the cloud droplet spectrum and crucially affects optical properties of clouds. This effect is still poorly understood (e.g., Brenguier and Grabowski 1993, Burnet and Brenguier 2007) and it is a significant source of uncertainty in aerosol indirect effects. As entrainment and mixing leads to the reduction of the liquid water content (LWC), the issue is whether the dilution of a cloud results in the reduction of only the droplet size (as in the homogeneous mixing), only the droplet concentration (as in the extremely inhomogeneous mixing), or both the concentration and the size (as in the inhomogeneous mixing). On the theoretical grounds, homogeneity of mixing depends on the relative magnitude of the time scales for droplet evaporation and turbulent homogenization. In the homogeneous mixing case, turbulent homogenization time scale needs to be much shorter than the droplet evaporation time scale. In the opposite limit, the extremely inhomogeneous mixing is thought to take place. This paper extends an approach for modeling subgrid-scale processes associated with entrainment and mixing proposed in Grabowski (2007; hereinafter G07) and Jarecka et al. (2009; hereinafter JGP09). In G07 and JGP09, the discussion was limited to the bulk representation of cloud microphysics. Here, the approach presented in G07 and JGP09 is extended to the double-moment bulk microphysics scheme of Morrison and Grabowski (2007; 2008) to locally *predict* the homogeneity of mixing.

The next section summarizes an approach to delay LWC evaporation (until the subgrid-scale homogenization can be assumed) developed in G07 and

JGP09. JGP09 referred to this approach as the $\lambda - \beta$ sunbrid-scale mixing model. Section 3 outlines the new approach that combines the $\lambda - \beta$ model with the double-moment bulk microphysics scheme of Morrison and Grabowski (2008, MG08 hereinafter) to locally predict the homogeneity of mixing. Section 4 presents an example of results from simulations of a field of shallow convective clouds with the new approach.

2. MODELING EVAPORATION OF CLOUD WATER RESULTING FROM ENTRAINMENT AND MIXING

The essence of the approach developed in G07 and JGP09 is to supplement the standard thermodynamic grid-averaged equations for the bulk advection-diffusion-condensation problem:

$$\frac{\partial \theta}{\partial t} + \frac{1}{\rho_o} \nabla \cdot (\rho_o \mathbf{u} \theta) = \frac{L_v \theta_e}{c_p T_e} C + D_\theta, \quad (1a)$$

$$\frac{\partial q_v}{\partial t} + \frac{1}{\rho_o} \nabla \cdot (\rho_o \mathbf{u} q_v) = -C + D_v, \quad (1b)$$

$$\frac{\partial q_c}{\partial t} + \frac{1}{\rho_o} \nabla \cdot (\rho_o \mathbf{u} q_c) = C + D_c, \quad (1c)$$

(where θ , q_v and q_c are the potential temperature, the water vapor and cloud water mixing ratios; $\rho_o(z)$ is the base state density profile; $\theta_e(z)$ and $T_e(z)$ are the environmental potential temperature and temperature profiles; \mathbf{u} is the wind velocity vector; L_v and c_p denote the latent heat of condensation and specific heat at constant pressure, respectively; C is the condensation rate, D terms represent subgrid-scale turbulent transport terms) with the evolution equations for the scale (or width) of cloudy filaments

λ and the fraction of the gridbox containing cloudy air β . The evolution of λ is supposed to represent the progress of subgrid-scale turbulent mixing toward the microscale homogenization (e.g., Broadwell and Breidenthal 1982, Jensen and Baker 1989). Local values of the cloudy-air fraction β are affected by resolved advection and subgrid-scale diffusion, and by the subgrid-scale homogenization. When extended into the multidimensional framework and written in the conservative (flux) form analogous to (1), the equation for λ and β are:

$$\frac{\partial \lambda}{\partial t} + \frac{1}{\rho_o} \nabla \cdot (\rho_o \mathbf{u} \lambda) = -\gamma(\epsilon \lambda)^{1/3} + S_\lambda + D_\lambda, \quad (2a)$$

$$\frac{\partial \beta}{\partial t} + \frac{1}{\rho_o} \nabla \cdot (\rho_o \mathbf{u} \beta) = S_\beta + D_\beta, \quad (2b)$$

where the first term on the right-hand side of (2a) describes the decrease of λ as the turbulent mixing progresses [ϵ is the local dissipation rate of the turbulent kinetic energy (TKE) and $\gamma \sim 1$ is a nondimensional parameter taken as $\gamma = 1.8$; see G07 and JGP09], S_λ , S_β are the source/sink terms, and D_λ , D_β are the subgrid transport terms analogous to D terms in (1). The source/sink terms S_λ and S_β consider three processes that affect the scale λ and the cloudy-air fraction β : (a) initial formation of a cloudy volume due to grid-scale condensation, (b) removal of a cloudy volume due to complete evaporation of cloud water, and (c) homogenization of a cloudy volume. A uniform cloudy gridbox is characterized by $\lambda = \Lambda$ and $\beta = 1$, where $\Lambda \equiv (\Delta x \Delta y \Delta z)^{1/3}$ (Δx , Δy , Δz are model gridlength in x , y , and z direction, respectively). A cloud-free gridbox has $\lambda = 0$ and $\beta = 0$. It follows that the source/sink term S_λ resets the current value of λ to Λ in cases (a) and (c), or resets λ to 0 in the case (b). Similarly, the source/sink term S_β resets the current value of β to 1 in cases (a) and (c), or resets β to 0 in the case (b). Microscale homogenization of a cloudy gridbox is assumed once the scale predicted by (2a) falls below the threshold value λ_0 taken as 1 mm (note that $\lambda_0 = 1$ cm was used in G07 and JGP09).

The overall motivation behind the approach is to represent the chain of events characterizing turbulent mixing—from the initial engulfment of the ambient fluid by an entraining eddy to the small-scale homogenization—and to include a corresponding delay in the bulk-model saturation adjustment until the gridbox can be assumed homogenized (see discussion in G07 and Fig. 1 in JGP09).

3. PREDICTION OF THE HOMOGENEITY OF MIXING IN A DOUBLE-MOMENT MICROPHYSICS SCHEME

In a LES model applying double-moment microphysics, both the cloud droplet concentration and the corresponding mixing ratio are predicted. Hence, unlike in Slawinska et al. (2008), it is possible to consider a prediction of the mixing scenario during turbulent mixing between cloudy air and subsaturated cloud-free air. In the MG08 double-moment scheme, the mixing scenario is determined by a single parameter α . This parameter is used to calculate the final droplet concentration after entrainment and turbulent mixing according to:

$$N^f = N^i \left(\frac{q_c^f}{q_c^i} \right)^\alpha, \quad (3)$$

where N^f is the final droplet concentration after microphysical adjustment due to evaporation, N^i is the droplet concentration after advection and turbulent mixing (i.e., the initial value for the microphysical adjustment), and q_c^i and q_c^f are the initial and final cloud water mixing ratios (i.e., before and after the microphysical adjustment). Note that, in the MG08 scheme, the microphysical adjustment of the cloud water mixing ratio q_c takes place before adjusting N , and it is dictated by the predicted supersaturation and characteristics of the cloud droplet population (i.e., the droplet concentration and size). Thus, q_c^i and q_c^f in (3) are already known, and (3) predicts the corresponding microphysical adjustment of the droplet concentration N once α is known. The parameter α varies from 0 for the case of homogeneous mixing (i.e., no change to N) to 1 for the extremely inhomogeneous mixing (i.e., when N changes in the same proportion as q_c and thus the mean volume radius remains unchanged). In simulations presented in MG08, α could only be assumed constant in space and time during the simulation. The goal of the developments reported here is to predict α locally at every gridbox within the cloud.

In the bulk $\lambda - \beta$ model discussed in JGP08 and in G07, the evaporation of cloud water due to turbulent mixing was delayed until the predicted filament scale λ reached the scale of molecular homogenization λ_0 . However, one might anticipate a gradual increase of the evaporation as the scale of λ_0 is approached instead of an abrupt transition from zero to finite evaporation. This is supported by simulations using the DNS approach (Andrejczuk et al. 2004, 2006) and simulations using the linear eddy model (e.g., Krueger 1993; Krueger et al. 1997; S. Krueger, personal communication). This is also consistent

with a heuristic argument that, during the turbulent stirring, complete evaporation of cloud droplets is anticipated near the edges of the filaments, while droplets away from the interface should not experience any evaporation at all (except due to resolved vertical motions). To include a gradual increase on the evaporation due to turbulent mixing, we postulate that the amount of cloud water Δq_c^* that evaporates at the filament edges is a fraction of the cloud water mixing ratio Δq_c that would evaporate during model time step in a traditional model, that is, when the microphysical adjustment is applied without any subgrid-scale considerations (i.e., applying model-predicted values of θ , q_v , N , and q_c). Heuristic arguments following ideas discussed in Sreenivasan et al. (1989) and Malinowski and Zawadzki (1993) and considering the increase of the surface area of the cloud-clear air interface during turbulent stirring suggest that

$$\Delta q_c^* = \frac{\lambda_0}{\lambda} \Delta q_c . \quad (4)$$

As expected, (4) implies almost no evaporation when $\lambda \gg \lambda_0$ and the correct evaporation $\Delta q_c^* \rightarrow \Delta q_c$ when $\lambda \rightarrow \lambda_0$. The cloud water mixing ratio Δq_c^* predicted by (4) is then used in (3) because $q_c^f \equiv q_c^i + \Delta q_c^*$. Note that the above considerations apply only for gridpoints affected by the entrainment and mixing, that is, when $\Delta q_c < 0$ and $\lambda < \Lambda$.

To predict the local value of α , we take advantage of the direct numerical simulations (DNS) results reported in Andrejczuk et al. (2009; hereinafter AGMS09). AGMS09 performed 72 simulations of decaying moist turbulence mimicking turbulent mixing and microscale homogenization of cloudy and clear air using detailed (bin) microphysics. They analyzed DNS results in terms of the instantaneous change of microphysical characteristics versus the ratio between the turbulent mixing and droplet evaporation time scales. The change in the microphysical characteristics was measured by the slope δ of the line depicting the evolution of the total number of droplets plotted against the mean volume radius cubed, both normalized by the initial values, the $r - N$ diagram, applied in Andrejczuk et al. (2004, 2006). In this diagram, the homogeneous mixing corresponds to the horizontal line (i.e., changing droplet size without changing the number of droplets; $\delta = 0$). The vertical line (reduction of the number of droplets without changing the size; $\delta \rightarrow \infty$) implies extremely inhomogeneous mixing. Based on these simulations, a simple relationship between the ratio of the two time scales (i.e., droplet evaporation and turbulent homogenization) and the slope of the mix-

ing line δ was proposed (see Fig. 2 in AGMS09). The slope δ is related to the parameter α in (3). Since $q_c \sim N r^3$, (3) implies that $N \sim (r^3)^{\alpha/(1-\alpha)}$. It follows that the slope $\delta \equiv dN/d(r^3)$ equals $\alpha/(1-\alpha)$ which leads to

$$\alpha = \frac{\delta}{1+\delta} . \quad (5)$$

The slope δ can be estimated as a function of the ratio between time scales of turbulent homogenization τ_{mix} and of droplet evaporation τ_{evap} using the relationship proposed in AGMS09 (Fig. 2 therein). The turbulent homogenization time scale is calculated following AGMS09 as

$$\tau_{mix} = \lambda/u(\lambda) , \quad (6)$$

where $u(\lambda)$ is the characteristic velocity at spatial scale equal to the filament scale λ . It can be related to the model-predicted TKE as

$$u(\lambda) = (TKE)^{1/2}(\lambda/\Lambda)^{1/3} . \quad (7)$$

This relationship assumes inertial range scaling for subgrid-scale turbulence and considers TKE to be dominated by the eddies of scale Λ [i.e., $u(\Lambda) \sim (TKE)^{1/2}$]. The droplet evaporation time scale is estimated as

$$\tau_{evap} = \frac{r^2}{A(1-RH_d)} , \quad (8)$$

where r is the mean volume radius of cloud droplets (predicted by the double-moment microphysics scheme), RH_d is the relative humidity of the cloud-free portion of the gridbox, and $A \approx 10^{-10} \text{ m}^2\text{s}^{-1}$ is the constant in the droplet diffusional growth equation (i.e., $dr/dt = AS/r$, where $S = RH - 1$ is the supersaturation). RH_d can be estimated using the mean (model-predicted) relative humidity of a gridbox RH , and assuming that $RH = 1$ for the cloud part of the gridbox. These lead to

$$RH_d = \frac{RH - \beta}{1 - \beta} . \quad (9)$$

Once the values of the two time scales are derived, their ratio provides a prediction of the slope δ using the relationship suggested in AGMS09, and the parameter α can be calculated from (5) and subsequently applied in (3).

4. APPLICATION OF THE SUBGRID-SCALE MODEL TO BOMEX SHALLOW CONVECTION

The subgrid-scale microphysics model described above was included in the anelastic semi-Lagrangian

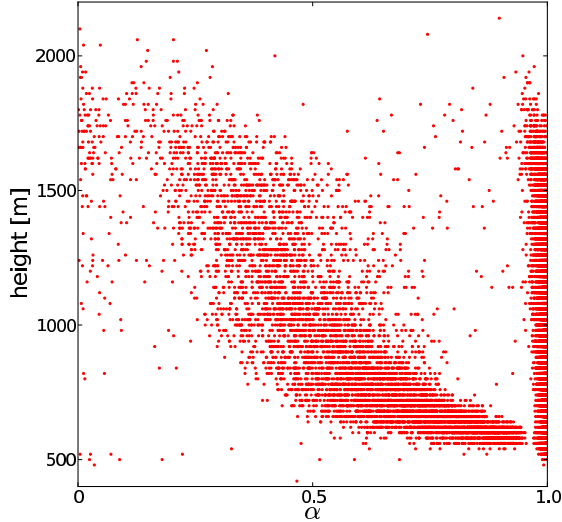


FIG. 1. Parameter α for the simulation with the new subgrid-scale model.

/Eulerian cloud model EULAG documented in Smolarkiewicz and Margolin (1997; model dynamics), Grabowski and Smolarkiewicz (1996; model thermodynamics), and Margolin et al. (1999; subgrid-scale turbulent mixing). Simulations of shallow convective clouds using the same setup as applied here and a single-moment microphysics were reported in Slawinska et al. (2008). The double-moment microphysics of Morrison and Grabowski (2007, 2008) was recently added to the model; simulations using the scheme and *prescribed* values of the parameter α will be reported in Slawinska et al. (2010; manuscript in preparation). Eulerian version of the model is used. The model simulates quasi-steady-state trade-wind shallow nonprecipitating convection observed during the Barbados Oceanographic and Meteorological Experiment (BOMEX; Holland and Rasmusson 1973) and used in the model intercomparison study described in Siebesma et al. (2003). In BOMEX observations, a 1.5 km-deep trade-wind convection layer overlays a 0.5 km-deep mixed layer near the ocean surface and lies under a 500 m-deep trade-wind inversion layer.

The cloud cover is about 10% and quasi-steady conditions are maintained by the prescribed large-scale subsidence, large-scale moisture advection, surface heat fluxes, and radiative cooling. Simulations with either prescribed α (0 or 1) or α calculated locally as described in the previous section are run

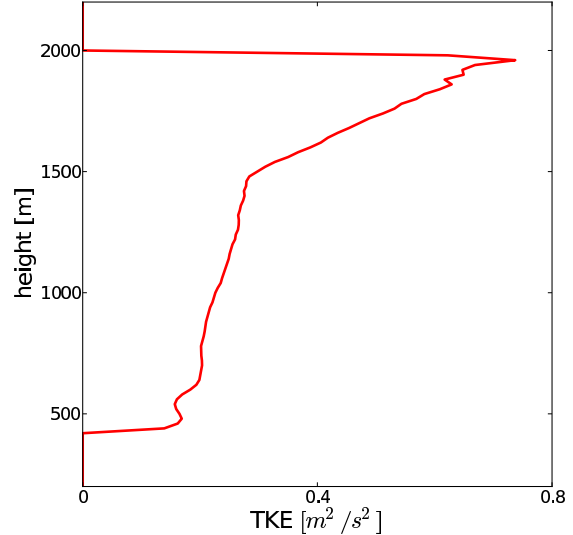


FIG. 2. Profile of the mean TKE in the simulation of Fig. 1.

for 6 hrs and data from last 3 hrs are used in the analysis. CCN characteristics are assumed as the PRISTINE case in MG08.

Figure 1 shows the scatter plot of α values as a function of height from the simulation where α is locally predicted. Only points with q_c exceeding 0.1 g kg^{-1} are included in the analysis. The figure shows that α values are grouped into two separate branches. The first branch represents mixing events close to the extremely inhomogeneous mixing (i.e., $\alpha \approx 1$). Additional analysis (not shown) suggests that such α values are typically found near cloud edges. This seems to agree with the analysis of aircraft observations reported in Small and Chuang (2010) following the methodology developed by Burnet and Brenguier (2007). Small et al. argued that at the cloud edge the extremely inhomogeneous mixing is dominant type of mixing. The second branch represents mixing events whose characteristics change from close to extremely inhomogeneous near the cloud base ($\alpha \approx 1$) to relatively close to homogeneous ($\alpha \approx 0$) near the cloud top.

The decrease of α observed in the second branch in Fig. 1 (i.e., the transition toward more homogeneous mixing in the upper parts of the cloud field) can be understood considering averaged profiles of the TKE and mean droplet radius. As illustrated in Figs. 2 and 3, both TKE and mean droplet radius increase with altitude. These make the turbulence

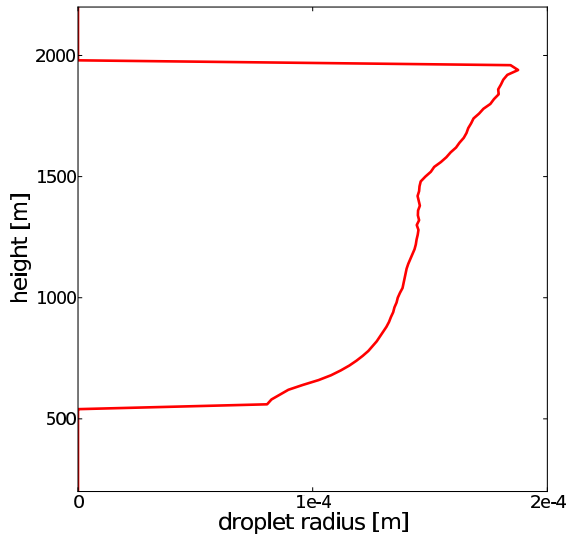


FIG. 3. Profile of the mean cloud droplet radius in the simulation of Fig. 1.

mixing more effective compared to droplet evaporation (i.e., reducing τ_{mix} and increasing τ_{evap}), so the mixing becomes more homogenous.

Finally, Fig. 4 compares profiles of the mean droplet number concentration between the simulation with α predicted and the simulations where α was fixed at 0 or 1 for the entire simulation (the latter as in Slawinska et al. 2010; manuscript in preparation). The mean concentrations are calculated as domain averages including only gridpoints with q_c exceeding 0.1 g kg^{-1} . As expected, the simulation with α predicted gives the mean concentration between the two extreme mixing scenarios. The differences between various scenarios are relatively small in the lower half of the cloud field, and they become more significant near the cloud field top. The latter may cause appreciable differences in radiative properties of the cloud field, an aspect currently under investigation.

Acknowledgments.

This work was supported by the European Union 6 FP IP EUCAARI (European Integrated Project on Aerosol Cloud Climate and Air Quality Interactions) No. 036833-2 and the Polish MNiSW grant 396/6/PR UE/2007/7. Additional support was provided by the NOAA grant NA08OAR4310543, DOE ARM grant DE-FG02-08ER64574, and by the NSF Science and Technology Center for Multi-Scale Mod-

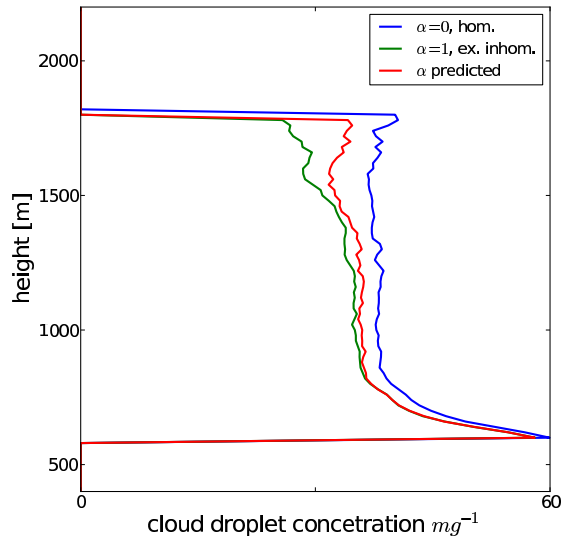


FIG. 4. Profiles of the droplet number concentration for the simulation with the new subgrid-scale model (red line) and for simulations assuming constant (in space and time) values of α , either 0 or 1 (blue and green lines, respectively).

eling of Atmospheric Processes (CMMAP), managed by Colorado State University under cooperative agreement ATM-0425247.

References

- Andrejczuk, M., W. W. Grabowski, S. P. Malinowski, and P. K. Smolarkiewicz, 2004: Numerical simulation of cloud-clear air interfacial mixing. *J. Atmos. Sci.*, **61**, 1726-1739.
- Andrejczuk, M., W. W. Grabowski, S. P. Malinowski, and P. K. Smolarkiewicz, 2006: Numerical simulation of cloud-clear air interfacial mixing: Effects on cloud microphysics. *J. Atmos. Sci.*, **63**, 3204-3225.
- Andrejczuk, M., W. W. Grabowski, S. P. Malinowski, and P. K. Smolarkiewicz, 2009: Numerical simulation of cloud-clear air interfacial mixing: Homogeneous versus inhomogeneous mixing. *J. Atmos. Sci.* **66**, 2493-2500.
- Brenguier, J.-L. and W. W. Grabowski, 1993: Cumulus entrainment and cloud droplet spectra: A numerical model within a two-dimensional dynamical framework. *J. Atmos. Sci.*, **50**, 120136.
- Broadwell, J. E., and R. E. Breidenthal, 1982: A simple model of mixing and chemical reaction in turbulent shear layer. *J. Fluid. Mech.*, **125**, 397-410.

- Burnet, F. and J. L. Brenguier, 2007: Observational study of the entrainment-mixing process in warm convective clouds. *J. Atmos. Sci.*, **64**, 1995-2011.
- Grabowski, W. W., 2007: Representation of turbulent mixing and buoyancy reversal in bulk cloud models. *J. Atmos. Sci.*, **64**, 3666-3680.
- Grabowski, W. W., and P. K. Smolarkiewicz, 1996: On two-time-level semi-Lagrangian modeling of precipitating clouds. *Mon. Wea. Rev.* **124**, 487-497.
- Holland, J. Z., and E. M. Rasmusson, 1973: Measurements of the atmospheric mass, energy, and momentum budgets over a 500-kilometer square of tropical ocean. *Mon. Wea. Rev.* **101**, 44-55.
- Jarecka, D., W. W. Grabowski, H. Pawlowska, 2009: Modeling of subgrid scale mixing in large-eddy simulation of shallow convective, *J. Atmos. Sci.*, **66**, 2125-2133
- Jensen, J. B., and M. B. Baker, 1989: A simple model for droplet spectral evolution during turbulent mixing. *J. Atmos. Sci.*, **46**, 2812-2829.
- Krueger, S. K., 1993: Linear-eddy modeling of entrainment and mixing in stratus clouds. *J. Atmos. Sci.*, **50**, 3078-3090.
- Krueger, S. K., C.-W. Su, and P. A. McMurthy, 1997: Modeling entrainment and fine-scale mixing in cumulus clouds. *J. Atmos. Sci.*, **54**, 2697-2712.
- Malinowski, S. P., and I. Zawadzki, 1993: On the surface of clouds. *J. Atmos. Sci.*, **50**, 5-13.
- Margolin, L. G., P. K. Smolarkiewicz, and Z. Sorbjan, 1999: Large-eddy simulations of convective boundary layers using nonoscillatory differencing. *Physica D*, **133**, 390-397.
- Morrison, H., and W. W. Grabowski, 2007: Comparison of bulk and bin warm rain microphysics models using a kinematic framework. *J. Atmos. Sci.*, **64**, 2839-2861.
- Morrison, H., and W. W. Grabowski, 2008: Modeling supersaturation and subgrid-scale mixing with two-moment bulk warm microphysics. *J. Atmos. Sci.*, **65**, 792-812.
- Siebesma, A. P., and Coauthors, 2003: A large eddy simulation intercomparison study of shallow cumulus convection. *J. Atmos. Sci.*, **60**, 1201-1219.
- Slawinska, J., W. W. Grabowski, H. Pawlowska, and A. A. Wyszogrodzki, 2008: Optical properties of shallow convective clouds diagnosed from a bulk-microphysics large-eddy simulation. *J. Climate*, **21**, 1639-1647.
- Small, J. D., and P. Y. Chuang, 2010: An analysis of entrainment mixing processes in warm cumulus. *13th Conference on Cloud Physics*, Portland, USA
- Smolarkiewicz, P. K., and L. G. Margolin, 1997: On forward-in-time differencing for fluids: An Eulerian/semi-Lagrangian nonhydrostatic model for stratified flows. *Atmos.-Ocean Special*, **35**, 127-152.
- Sreenivasan, K. R., R. Ramshankar, and C. Meneveau, 1989: Mixing, entrainment and fractal dimensions of surface in turbulent flows. *Proc. R. Soc. Lond.*, **A421**, 79-108.